ACS OMEGA

http://pubs.acs.org/journal/acsodf

Article

Xe Adsorption on Noble Metal Clusters: A Density Functional Theory Investigation

Arnaud Monpezat, Jean Aupiais, and Bruno Siberchicot*

Cite This: *ACS Omega* 2021, 6, 31513−31519

Read Online

ACCESS | Metrics & More | Article Recommendations | Supporting Information

ABSTRACT: The adsorption mechanism of xenon on three noble metal clusters (M = Ag, Au, and Cu) has been investigated in the framework of density functional theory (DFT) within generalized gradient approximation (GGA-PBE). The *ab initio* calculations were performed with the quantum molecular dynamics (QMD) package ABINIT using the projector augmented (PAW) formalism. The spin−orbit coupling (SOC) and dispersion effects (Van der Waals DFT-D3) have been taken into account. According to these calculations, the M−Xe bonds are partly covalent and electrostatic and their contribution depends on the cluster size and nature. This study underlines the importance of using the SOC and the Van der Waals (VdW) effects. Based on these results, copper nanoparticles have the highest affinity for interaction with xenon compared with silver and gold.

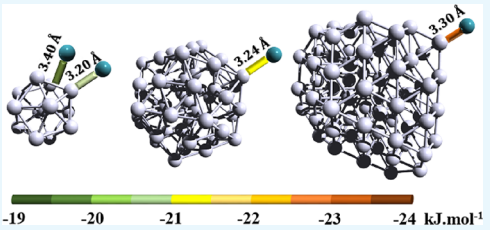

I. INTRODUCTION

Adsorption of xenon is a commonly studied phenomenon because this noble gas is not only rare and expensive but is also very useful in various applications such as lighting, medicine, and propulsion of spatial devices or even in monitoring worldwide nuclear activities.[1−4] Due to its electronic structure and its weak interactions with other atoms, this noble gas is also used to study material surfaces.[5] In parallel, metal-supported catalysts are nowadays widely used in industrial applications to improve process efficiency.[6−10] To optimize specific surfaces, metals are generally dispersed in the form of nanoparticles.[11] Silver nanoparticles are used in adsorption processes to trap radioactive xenon in nuclear activity monitoring. The evolution of these nanoparticles is therefore genuinely surveyed to optimize adsorption performances and avoid its progressive deactivation.[12,13] Indeed, the size of the metallic nanoparticles is critical for xenon capture, and the investigations of Deliere *et al.*[14] have revealed that the mean particle size is centered around 1 nm. Before starting larger-scale modeling and testing with new materials, first simulations were necessary on small clusters to compare the phenomena involved. The first results and the importance of the various parameters will orient research toward specific materials.

In this work, we suggest to examine the interaction of xenon and transition metal nanoclusters/nanoparticles.

In first studies, the interaction between xenon and metal surfaces has been described as a pure Van der Waals interaction.[15] Using empirical potentials such as Lennard-Jones potential, the high-coordination sites of the surfaces (also called hollow sites) were favored. At this time, experimental and theoretical studies seemed to reveal that noble gases would adsorb preferentially on hollow sites because they maximize Van der Waals interactions.[15]

However, this widely accepted theory has then been queried with different studies about xenon adsorption on Pt(111) surfaces.[16] Indeed, these investigations concluded that the low-coordination site (also called the on-top site) was preferred for this metal. Figure 1 represents the two potential sites for the bonding between a metal atom and a metallic cluster.

Numerous theoretical and experimental studies have then confirmed the on-top site preference for Cu(111), Pd(111), Ru(0001), and Pt(111). Whereas the hollow-site bonding would be characteristic of a Van der Waals interaction, the on-top site can be explained, assuming a chemical contribution to the bond.[16,17]

Regarding more details, different studies have first highlighted the important role played by the spin−orbit coupling (SOC) and described the effect of the splitting of Xe 5p states into $5p_{1/2}$ and $5p_{3/2}$ on the metal−Xe interaction.[16] Then, the bond has been attributed to a charge transfer from the 5p orbital of the adsorbate to some unoccupied metal d orbitals sitting just above the Fermi energy, with the metallic d_z^2 orbital playing a prominent role in the bonding mechanism.[16] Whereas the spin−orbit effect was responsible for the first splitting of Xe 5p orbitals, an extra splitting of the $5p_{3/2}$ orbitals of xenon was observed. This evolution is attributed to the reduction in local symmetry on adsorption. This effect was observed in photoemission measurements and is characterized

Received: July 20, 2021
Accepted: October 27, 2021
Published: November 17, 2021

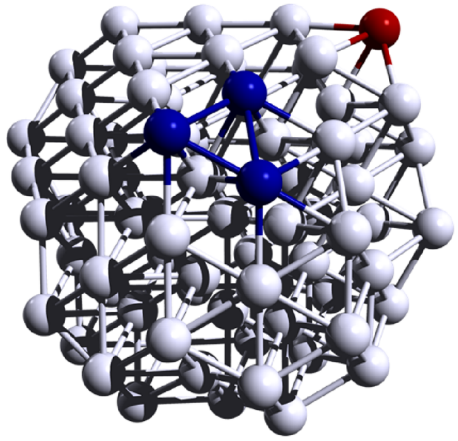

Figure 1. Illustration of the two potential sites for a binding between a xenon atom and a metallic cluster Ag_79: the on-top site is represented in red (low coordination) and the hollow site (high coordination) is in blue.

by a broadening of the $5p_{3/2}$ level for Xe in a monolayer of Xe adsorbed on a plane surface of W(001)[18] and Pd (001).[19] Two origins of this splitting were postulated: the interaction between the adatom and the substrate and the interaction within the xenon layer. The three effects have been quantified according to their magnitude. The spin−orbit coupling produces the greatest effect followed by the Xe−Xe interactions and, finally, the small contribution from the Xe−adsorbate interactions.[20] Then, the Van der Waals attraction acts in the second step. The energy level splitting of a xenon atom adsorbed on a silver surface is shown in Figure S-1, Supporting Information.

Finally, while all of these previous studies pointed out the importance of different effects—spin−orbit coupling, Xe $5p_{3/2}$ splitting, and Van der Waals interaction—on adsorption phenomena, very few of them have included both these parameters in their calculations.[16,21] It was even postulated that the M−Xe distances are short enough to be described exclusively by the GGA functional.[22] In this work, we have studied the interaction between xenon and transition metals (Cu, Ag, and Au) using both the spin−orbit effect and the dispersion correction to underline the impact of these two parameters. After having investigated the nature of the bond between xenon and silver for different sizes of clusters, the calculations were extended to gold and copper clusters. Beyond the knowledge of the different physical contributions to the bonding, we also determined the most efficient nanoclusters to adsorb xenon. A more practical goal of this work is to evaluate adsorption energies, which would be used in subsequent calculations of adsorption isotherms.

II. RESULTS

II.A. Xenon Adsorption on Silver Clusters. Starting from silver with the Ag_2 dimer, a calculation on a linear system in GGA leads to an equilibrium distance of Ag−Xe equal to 3.05 Å (adsorption energy ΔE_{ad} = −0.67 kJ·mol^{-1}). Including spin−orbit coupling and Van der Waals interaction, the distance of Ag−Xe increases to 3.15 Å with an energy ΔE_{ad} equal to −0.82 kJ·mol^{-1}. Performing *ab initio* calculations (DFT CAM-B3LYP), Jamshidi *et al.*[21] found an average distance d_{Ag-Xe} = 3.13 Å and ΔE_{ad} = −0.45 kJ·mol^{-1}. Without SOC and VdW, their results are in very good agreement with our calculations. By taking into account the spin−orbit coupling and VdW, our adsorption energy is reinforced.

Continuing with the 13-atom cluster (Ag_13), we calculate the adsorption of Xe, considering the different levels of approximation available in our calculations, *i.e.*, GGA, GGA + SOC, and GGA + SOC + Van der Waals. The decomposition of the different physical effects allows shedding some light on their respective importance.

Table 1 and Figure 2 show the Ag_13 cluster and the two possible sites (hollow and on-top sites) and the evolution of the equilibrium values depending on the ingredients used in the calculations (GGA, SOC, and VdW), respectively.

Table 1. Evolution of the Adsorption Energy with Different Parameters Used in Calculations for the Ag_13 Cluster (Hollow and On-Top Sites)

site	hollow site		on-top site	
equilibrium value	distance of Ag−Xe (Å)	energy (kJ·mol^{-1})	distance of Ag−Xe (Å)	energy (kJ·mol^{-1})
GGA				
GGA + SOC	4.4	−2.0	3.2	−7.5
GGA + SOC + VdW	3.4	−19.7	3.2	−21.0

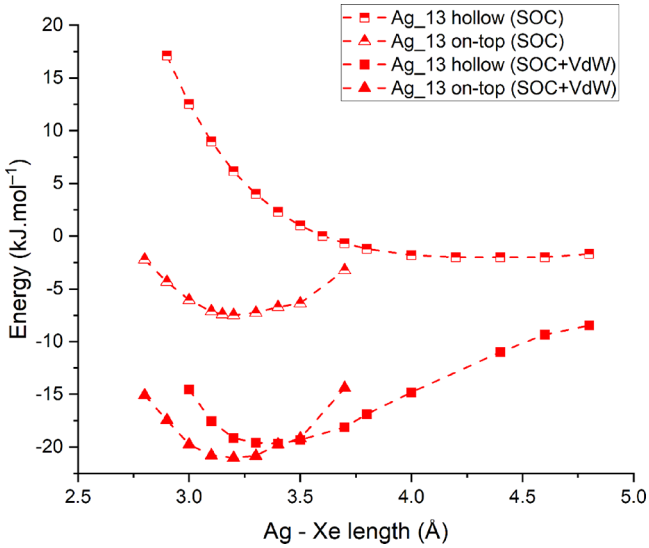

Figure 2. Energy of the bond as a function of the length of Ag−Xe for the 13-atom silver cluster at hollow and on-top sites with and without the dispersion correction.

The validity of the static approximation has been confirmed with an atomic relaxation of the cluster Ag_13 with Xe on the top site. The distance of Ag (central)−Ag (facing Xe) decreases by 1.4%; the adsorption energy varies from 0.41 kJ·mol^{-1} to about 20 kJ·mol^{-1}. Our static approximation seems justified.

Based on these results, it is possible to make assumptions about the nature of the interaction between xenon and silver nanoclusters. Indeed, the favored on-top site suggests the presence of a chemical contribution as highlighted in the literature, as a pure physical Van der Waals interaction would have been stabilized in the hollow site.

Moreover, the densities of state (DOS) obtained for xenon, silver, and the combination revealed not only the first splitting of the 5p xenon orbitals but also an extra splitting of circa 0.7

https://doi.org/10.1021/acsomega.1c03849
ACS Omega 2021, 6, 31513−31519

eV due to the metal interaction as mentioned in the literature.[16] The spin−orbit coupling constant of Xe has been calculated and is 1.22 eV. Based on these DOS, two contributions can be distinguished: the orbital recovery of the xenon 5p and silver 5d and the modification of the DOS for xenon when it interacts with silver. The DOS obtained are displayed in Figure S-1, Supporting Information. The addition of the dispersion correction has a non-negligible impact on the energies as it is represented in Figure 2.

This effect of dispersion forces does not drastically change the bond length, but the energy is shifted from −7.5 kJ·mol^{-1} to −21.0 kJ·mol^{-1}. Indeed, this physical contribution adds an important and non-negligible stability to this Xe−Ag_13 system.

The silver−xenon bonding is favored on the on-top site, which is coherent with the literature.[16] The lengths and energies of these bonds for the two sites are nevertheless very close: less than 2 kJ·mol^{-1} of difference.

The interatomic interactions can be analyzed through the topological analysis of the electron density distribution $\rho(r)$. According to Bader's QTAIM (Quantum Theory of Atoms in Molecules),[23] a chemical bonding can be characterized by the existence of a critical point (BCP) and the corresponding bond path. Its nature is revealed by descriptors at the BCP such as the electron density $\rho(r_c)$, Laplacian $\nabla^2\rho(r_c)$, and total energy density $H(r_c)$, permitting a comprehensive characterization from strong shared-shell to weak closed-shell interatomic interactions depending on the sign of the Laplacian.

Concerning the Ag−Xe interaction in the Ag_13 cluster, the electron density at BCP is weak (∼0.02 a.u.), Laplacian is positive (∼0.04 a.u.), and $H(r_c)$ is slightly negative (∼−0.08 a.u.). This set of descriptors suggests a partially electrostatic and partially covalent interaction.

The bond has then been studied depending on the cluster size for the favored position: the on-top site (linear configuration Ag−Ag−Xe for the dimer). Figure 3 presents the evolution of the bonding energy as a function of the cluster size for the low-coordination site.

The binding energy is greater for the silver cluster of 79 atoms and its bond length is longer. Indeed, while the energy of the Ag_13 cluster is −21.00 kJ·mol^{-1} with a bond length of 3.2 Å, the one of Ag_79 is −23.07 kJ·mol^{-1}, and the bond length is 3.3 Å. This value is lower than 3.72 Å (experimental, 3.54 Å),[24] which is the distance determined when Xe is adsorbed on a surface.[16] This result means that the bond between xenon and silver is favored for a bigger nanoparticle. More calculations should be done with greater cluster sizes to confirm this behavior.

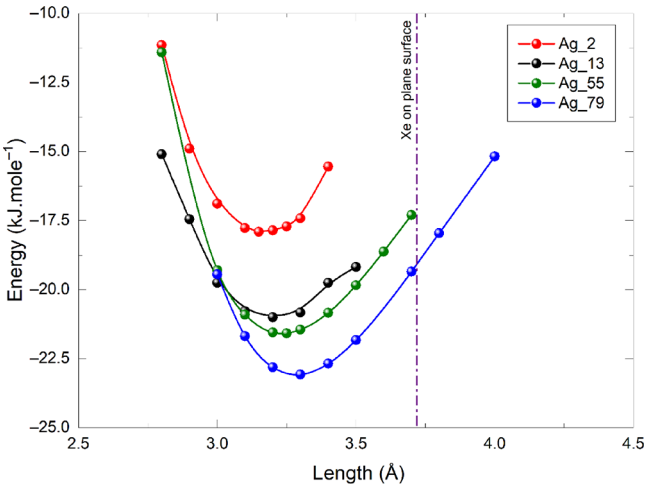

Figure 3. Energy of the bond as a function of the length of Ag−Xe for the 2-, 13-, 55-, and 79-atom silver clusters at the on-top site, with the dispersion correction (VdW). The adsorption occurs on a plane at 3.72 Å.[16]

For the Ag_79 cluster, the physical contribution becomes the most important one so that the bond energy changes from −1.8 kJ·mol^{-1} (at 4.6 Å) to −23.07 kJ·mol^{-1} (at 3.3 Å). In this case, the addition of the dispersion correction changes the energy but also the length of the bond: the physical contribution became more important for this bigger cluster.

The same behavior can be observed with the two sites, and the physical contribution (dispersion correction) also plays an important role for the high-coordination site (hollow site), as expected.

The literature only presents results of adsorption of Xe layers on metal surfaces. To summarize, the energy for (111) silver surfaces is measured between −21.74 and −17.31 kJ·mol^{-1}[24−29] with bond lengths between 3.68 and 3.74 Å. These data are coherent with our results.

These results indicate that the spin−orbit effect and the dispersion correction cannot be neglected to study the interaction between xenon and transition metals like silver. The importance of spin−coupling effect on atomization energies and structures of gold clusters were previously pointed out.[30,31] Our work suggests that this contribution is also of key importance to quantify the adsorption phenomenon of Xe on noble metals. As already observed by Jamshidi *et al.*,[21] the binding of noble metal clusters with rare gas has both physical and chemical contributions. The bond length is shorter than the sum of the two Van der Waals radii (Ag: 1.72 Å; Xe: 2.16 Å; Σ = 3.88 Å) and is intermediate between conventional covalent and Van der Waals interactions. The Bader analysis confirmed that both contributions are present.

II.B. Xenon Adsorption on Noble Metal Clusters. To complete this study, we have investigated the bond between xenon and two other transition metals: gold and copper (Figure 4). To facilitate the study, we have limited the study to the 13-atom cluster.

To complete with literature data, the adsorption energy for gold (111) surfaces is −20.58 kJ·mol^{-1},[32] and for Cu, it varies between −17.596 and −26.923 kJ·mol^{-1}[32,33] with bond lengths between 3.20 and 3.60 Å.

The copper cluster highlights the lowest binding energy together with the shortest M−Xe bond followed by gold and silver. As the Van der Waals contribution to the total energy varies as the atomic polarizability (Cu: 47 a.u.; Ag: 55 a.u.; Au: 36 a.u.), the strength of the chemical bond is essential to determine the total energy as well as the bond length. More generally, the shorter the bond, the stronger the interaction. For a similar bond length, the energy is rather the same regardless of the metal.

III. DISCUSSION

The only known and neglected property in this study is the magnetic effect of silver nanoclusters. This parameter has been set aside to lighten calculations.

This peculiar type of bonding between a noble metal and xenon leads us to think about the aurophilic or metallophilic

https://doi.org/10.1021/acsomega.1c03849
ACS Omega 2021, 6, 31513−31519

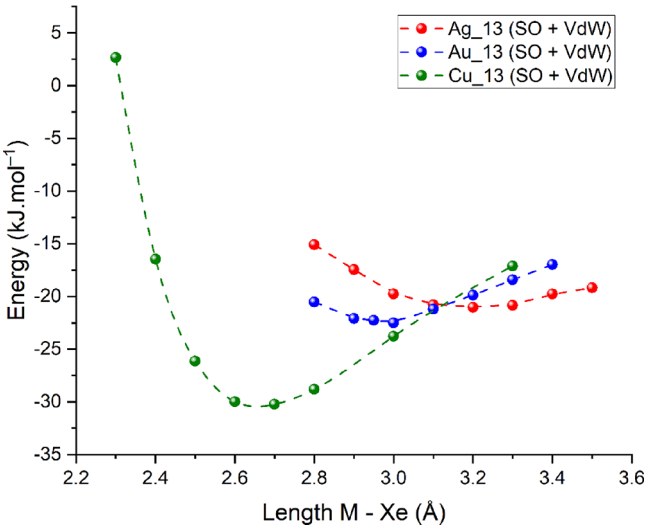

Figure 4. Energy of the bond as a function of the length of M−Xe for the 13-atom clusters of silver, copper, and gold, at the on-top site, obtained by calculation with SOC and dispersion correction.

attraction.[34] It seems pertinent to compare the two kinds of chemical bondings.

In some low-coordinate gold-based organometallics, short direct bonds have been observed between gold atoms. The gold atoms approach each other to an equilibrium distance of around 3 Å with a small energy between −21 and −46 kJ·mol^{-1}.[35] Relativistic effects explain this surprising attraction. Two main hypotheses were made: (i) a pure correlation effect strengthened by relativistic effects[35] and (ii) relativistic modifications of the gold valence bands, which bring the 5d and 6s orbitals into close energetic proximity, leading to 6s/5d hybridization.[36] This phenomenon leads to systems with unusual conformations in which gold atoms are the nearest neighbors. Similar kinds of bonds are also found between other closed-shell metals such as copper or silver with generally weaker bonds (metallophilicity). Based on the similar characteristics, the aurophilic interaction was put in the same category as standard hydrogen bonding.

In both experiments, aurophilic/metallophilic and noble metal−Xe interactions, the basic feature responsible for the interaction is mainly relativistic. In both cases, the results are close, *i.e.*, the same order of magnitude for the bond length (around 3 Å; intermediate between covalent and Van der Waals) and comparable weak bonding energy. The difference seems to come from the importance of one type of involved relativistic effect; the xenon atom in our case introduces a strong spin−orbit coupling. In our clusters, the main effect comes from the splitting of the Xe 5p states into $5p_{1/2}$ and $5p_{3/2}$ due to spin−orbit coupling with an additional splitting of $5p_{3/2}$ orbitals in interaction with the metallic d_z^2 orbital of the formally closed-shell metal substrate.

As stated by Clarke *et al.*,[16] in a xenon layer adsorbed on a silver plane, the total splitting of Xe 5p states is caused by both lateral interactions in the layer and substrate−adsorbate interactions. This additional splitting of $5p_{3/2}$ is already observed on an isolated Xe_2 dimer[37] (d_{Xe-Xe} = 4.60 Å). To complete this work, it seems important to make new simulations with a complete layer of xenon around a metal cluster.

In this way, it would be possible to quantify the Xe−Xe interactions on splitting and bond stability.

IV. CONCLUSIONS

Through this work, we have studied the adsorption mechanism of xenon on three noble metal clusters (M = Ag, Au, and Cu) in the framework of density functional theory (DFT) within generalized gradient approximation (GGA-PBE). The *ab initio* calculations were performed with the quantum molecular dynamics (QMD) package ABINIT using the projector augmented (PAW) formalism.

Spin−orbit coupling, Xe $5p_{3/2}$ splitting, and Van der Waals interaction have been taken into account to describe more accurately the adsorption phenomena, as had been brought to light by several previous studies.

First, we have constructed metallic clusters and our results are in good agreement with those of the literature.[38] For silver, the bond length starts around 2.50 Å for the dimer and stabilizes at around 2.85 Å for greater clusters. The bond length (and the bonding energy per atom) increases with the size of the system toward the bulk's value. Moreover, as expected for the three metallic clusters containing 13 atoms, the values are smaller than the nearest-neighbor distance found in their respective face-centered cubic crystal structure.

In the second part, starting from silver with the 13-atom cluster, we have calculated the adsorption of Xe, considering the different levels of approximation available in our calculations, *i.e.*, GGA, GGA + SOC, and GGA + SOC + Van der Waals. Based on these results, the favored on-top site suggests the presence of a chemical contribution. Moreover, the densities of state (DOS) obtained for xenon, silver, and the combination revealed not only the first splitting of the 5p xenon orbitals or the orbital recovery of the xenon 5p and silver 5d but also an extra splitting of circa 0.7 eV due to the metal interaction. The spin−orbit coupling constant of Xe has been calculated and is 1.22 eV. The addition of the dispersion correction has an important impact on the energies. Indeed, this physical contribution adds significant stability to this Xe−Ag system.

We have then extended this work to different clusters (2, 13, 55, and 79 atoms) for the on-top site. The binding energy (−23.07 kJ·mol^{-1}) is greater for the silver cluster of 79 atoms and its bond length is longer (3.3 Å). By comparison, the energy of the Ag_13 cluster is −21.00 kJ·mol^{-1} with a bond length of 3.2 Å. These results indicate that the bond between xenon and silver is favored for a bigger nanoparticle. The addition of the dispersion correction changes the energy but also the length of the bond: the physical contribution becomes more important for bigger clusters. These results indicate that the spin−orbit effect and the dispersion correction cannot be neglected to study the interaction between xenon and transition metals such as silver, which is confirmed by the Bader analysis.

In the third and final part, we have investigated the bond between xenon and two other transition metals, gold and copper, in limiting the framework to the 13-atom cluster and on-top site. The copper cluster highlights the lowest binding energy and the shortest M−Xe bond followed by gold and silver. The Van der Waals contribution to the total energy varies like the atomic polarizability (Cu: 47 a.u.; Ag: 55 a.u.; Au: 36 a.u.).

According to these calculations, the M−Xe bonds are partly covalent and electrostatic and their contribution depends on

https://doi.org/10.1021/acsomega.1c03849
ACS Omega 2021, 6, 31513−31519

the cluster size and nature. This study underlines the importance of using the SOC and the Van der Waals effects. Based on these results, copper nanoparticles have higher affinity for interaction with xenon than silver and gold.

It is finally possible to draw the parallel between the aurophilic/metallophilic effect and noble metal−Xe interaction as the basic feature responsible for the interaction is mainly relativistic. In both cases, the results are close in terms of bond length and energy. The difference seems to come from the importance of one type of involved relativistic effect, and the xenon atom in our case introduces a strong spin−orbit coupling.

V. THEORETICAL APPROACH

Ab initio calculation of metallic cluster structures and the M−Xe bond was performed with the quantum molecular dynamics (QMD) package ABINIT in the projector augmented wave formalism (PAW).[39,40] The first-principles total energy calculations were performed using the generalized gradient approximation density functional of Perdew, Burke, and Ernzerhof (GGA-PBE).[41] Scalar relativistic effects are taken into account and spin−orbit coupling (SOC) is included. The addition of Xe to the clusters has also been intensely studied: some experiments were performed with and without SOC and the Van der Waals effect was included according to the formalism of Grimme's semiclassical pairwise additive corrections of the D3 type for accurate calculations in DFT (DFT-D3).[42] The Brillouin zone was sampled with the Γ point only.

The pseudopotentials of xenon, silver, gold, and copper have been generated for the PBE exchange-correlation functional using the ATOMPAW code.[43] An adequate energy cutoff of 816 eV has been fixed for the pseudopotentials, and a convergence criterion of 0.02 Ha/Bohr has been chosen for the calculations to ensure fully converged forces for all systems.

It is known that small particles of transition metals could evidence weak magnetic moments even for nonmagnetic bulk metals such as silver.[44] This effect is particularly large in Ag_13 for which a magnetic moment of 5.0 μ_B (0.39 μ_B/atom) is calculated. The magnetization is expected to decrease (Ag_55: M = 3.0 μ_B, 0.054 μ_B/atom) for greater clusters. Performing a spin-polarized (SP) calculation on Ag_13 with one Xe atom adsorbed on a top site, we have not observed significant modification of the adsorption energy with and without SP (about 1 kJ·mol^{-1} on adsorption energy). Assuming that the magnetization has a weak effect on rare gas adsorption, it was not considered further in this work to avoid cumbersome calculations.

V.A. Choice of the Nanoparticles. Among the numerous sizes and shapes observed and studied for metal clusters, four silver clusters with different sizes have been selected to determine further the evolution of the adsorption of Xe. These Ag_n systems contain n = 2, 13, 55, and 79 atoms.

It has been a long time to ascertain the lowest-energy geometry and dimensionality of neutral clusters. According to the metal, planar configurations are adopted up to six or seven atoms; beyond that, they change from 2D to 3D structures. Numerous semi-empirical and band structure calculations have been performed to determine the ground-state geometry of such clusters even in dimensionality. For silver, it was shown[45] that the most stable geometry for the 13-atom cluster is a perfect icosahedron containing two layers, *i.e.*, 12 atoms in a layer and an additional atom in its center (I_h symmetry). Other geometries have also been proposed for the ground state: cuboctahedral (CO_h)[46] and "buckled bi-planar" (BPP−C_{2v} symmetry).[47] The Cu_13 cluster is described as a perfect icosahedron[46] but also BPP.[47] The Au_13 cluster can be icosahedral and BPP[47] and can be in a C_1-3D structure.[48] Most of the different calculations are summarized by Sun *et al.*[48] and this article pointed out the difficulty to determine exact ground-state geometry of such nanoclusters due to nearly degenerate isomers.

As we are not interested in the lowest-energy geometry determination of the clusters but in the metal−xenon interaction, we choose to consider only the same simple structure for all the 13-atom clusters, *i.e.*, the icosahedral geometry.

For clusters greater than 13 atoms, the number of layers is greater and the structure generally follows the crystalline arrangement of the bulk metal.[38,49] Arranging 55 atoms in a closed shell leads to (at least) three possible topologies: an icosahedron, a truncated decahedron, and a cuboctahedron. The lowest energy 55-isomer within this work is a closed-shell icosahedron, in agreement with previous DFT calculations. The 79-atom cluster is of FCC type and is a truncated octahedral object.[50]

For gold and copper clusters, the geometries are the same and we only focused on systems containing 13 atoms.

All the clusters have been built with a small arbitrary interatomic length and placed at the center of a cubic simulation supercell (Ag_2 and Ag_13: 15 Å; Ag_55 and Ag_79: 26 Å). These large boxes lead to negligible interactions between periodic images of clusters. Keeping the initial symmetry, an atomic relaxation was performed until an equilibrium was reached; we assumed that the convergence was achieved when the forces acting on the atoms did not exceed 0.02 Ha/Bohr. For a given cluster M_n, the binding energy per atom (BE) is defined as:

$$\mathrm{BE}(M_n) = [E_{\mathrm{tot}}(M_n) - nE(M_{\mathrm{atomic}})]/n$$

The results are gathered in Tables 1 and 2 for the different clusters. Some of the related data extracted from the literature are also presented for comparison.

Table 2. Binding Energies and Bond Lengths for the Three Metal Clusters (Cu, Ag, and Au)

	Cu_13	Ag_13	Au_13
E (kJ·mol^{-1})	−30.35	−21.00	−21.71
D_{M-Xe} (Å)	2.70	3.20	3.05

Our results are in good agreement with most of the data from the literature (Tables 3 and 4). For silver, the bond length starts at around 2.50 Å for the dimer and stabilizes at around 2.85 Å for greater clusters. In such nanoparticles, the bond length and the bonding energy per atom increase with the size of the system toward the bulk's value. It was shown for similar ruthenium nanoparticles[50] that many physical properties $X(n)$ scale with increasing nuclearities n following the expression $X(n) \approx k_X \cdot n^{-1/3}$, with k_X being a constant depending on the physical property considered.

As expected for the three metallic clusters containing 13 atoms, the values are smaller than the nearest-neighbor distance found in their respective face-centered cubic crystal structure: *i.e.*, Cu: d_{nn} = 2.5456 Å (a = 3.60 Å); Ag: d_{nn} = 2.8892 Å (a = 4.086 Å); Au: d_{nn} = 2.8837 Å (a = 4.0782 Å).

https://doi.org/10.1021/acsomega.1c03849
ACS Omega 2021, 6, 31513−31519

Table 3. Physical Properties of Silver Clusters Ag_n (n = 2, 13, and 79)

	Ag_2	Ag_13	Ag_55	Ag_79
bond length of Ag−Ag (Å)	2.57 (2.53)[51]	2.78 (2.87)[38]	2.73	2.86
binding energy (kJ·mol^{-1})	−88.85 (−99.21)[46]	−164.81 (141.1)[46]	−221	−226.74
D^a (nm)		0.6	∼0.9	∼1.2

[a]Mean diameter of the corresponding cluster.

Table 4. Physical Properties of M_13 (M = Ag, Au, and Cu) Clusters

	Cu_13	Ag_13	Au_13
bond length of M−M (Å)	2.44 (2.51)[52]	2.78 (2.87)[38]	2.76 (2.78)[53]
binding energy (kJ·mol^{-1})	−220.79 (−237)[52] (−206)[46]	−164.81 (141.1)[46]	−213.09 (−268.7)[53]

V.B. Adsorption of Xe on Metals: Simulation of the Bond M−Xe. For this study, only two positions of adsorption have been considered: the hollow site corresponding to a high coordination (interstitial site) and the on-top site corresponding to a low coordination (crystal top). To simulate the bond between a xenon atom and a metal cluster, one atom of the rare gas was positioned at a fixed distance from the considered site and a static calculation of energy was made for each position. The thermodynamic functions were extracted and the energies of M−Xe bonds were calculated:

$$\Delta E_{ad}(M - Xe) = H(M_n, Xe) - H(M_n) - H(Xe^{gas})$$

■ ASSOCIATED CONTENT

Supporting Information

The Supporting Information is available free of charge at https://pubs.acs.org/doi/10.1021/acsomega.1c03849.

Densities of state (DOS) obtained for xenon, silver, and the combination (PDF)

■ AUTHOR INFORMATION

Corresponding Author

Bruno Siberchicot − *CEA, DAM, DIF, F-91297 Arpajon, France; Université Paris-Saclay, CEA, Laboratoire Matière en Conditions Extrêmes, F-91680 Bruyères-le-Châtel, France*; Email: bruno.siberchicot@cea.fr

Authors

Arnaud Monpezat − *CEA, DAM, DIF, F-91297 Arpajon, France*; orcid.org/0000-0002-2288-384X

Jean Aupiais − *CEA, DAM, DIF, F-91297 Arpajon, France*; orcid.org/0000-0003-2830-4447

Complete contact information is available at: https://pubs.acs.org/10.1021/acsomega.1c03849

Notes

The authors declare no competing financial interest.

■ ACKNOWLEDGMENTS

The authors are sincerely thankful to Pr. Bruno Chaudret, Pr. Laurent Maron, and Pr. Romuald Poteau for their comments on an earlier version of the manuscript. These discussions have improved our work and broadened the study to include the metallophilic phenomena.

■ REFERENCES

(1) Stanley, R. E.; Moghissi, A. A. *Noble Gases*; U.S. Environmental Protection Agency: 1975.

(2) Sanders, R. D.; Ma, D.; Maze, M. Xenon: Elemental Anaesthesia in Clinical Practice. *Br. Med. Bull.* **2005**, *71*, 115−135.

(3) Fontaine, J. P.; Pointurier, F.; Blanchard, X.; Taffary, T. Atmospheric Xenon Radioactive Isotope Monitoring. *J. Environ. Radioact.* **2004**, *72*, 129−135.

(4) Topin, S.; Greau, C.; Deliere, L.; Hovesepian, A.; Taffary, T.; Le Petit, G.; Douysset, G.; Moulin, C. SPALAX New Generation: New Process Design for a More Efficient Xenon Production System for the CTBT Noble Gas Network. *J. Environ. Radioact.* **2015**, *149*, 43−50.

(5) Raftery, D. Xenon NMR Spectroscopy. In *Annual Reports on NMR Spectroscopy*; Webb, G. A. Ed.; Academic Press: 2006; Vol. *57*, pp. 205−270, DOI: 10.1016/S0066-4103(05)57005-4.

(6) Jiang, Z.-J.; Liu, C.-Y.; Sun, L.-W. Catalytic Properties of Silver Nanoparticles Supported on Silica Spheres. *J. Phys. Chem. B* **2005**, *109*, 1730−1735.

(7) Schauermann, S.; Nilius, N.; Shaikhutdinov, S.; Freund, H.-J. Nanoparticles for Heterogeneous Catalysis: New Mechanistic Insights. *Acc. Chem. Res.* **2013**, *46*, 1673−1681.

(8) Mondloch, J. E.; Bayram, E.; Finke, R. G. A Review of the Kinetics and Mechanisms of Formation of Supported-Nanoparticle Heterogeneous Catalysts. *J. Mol. Catal. Chem.* **2012**, *355*, 1−38.

(9) Huang, N.; Xu, Y.; Jiang, D. High-Performance Heterogeneous Catalysis with Surface-Exposed Stable Metal Nanoparticles. *Sci. Rep.* **2015**, *4*, 7228.

(10) Dong, X.-Y.; Gao, Z.-W.; Yang, K.-F.; Zhang, W.-Q.; Xu, L.-W. Nanosilver as a New Generation of Silver Catalysts in Organic Transformations for Efficient Synthesis of Fine Chemicals. *Catal. Sci. Technol.* **2015**, *5*, 2554−2574.

(11) Bailie, J. E.; Hutchings, G. J.; O'Leary, S. Supported Catalysts. In *Encyclopedia of Materials: Science and Technology*; Buschow, K. H. J.; Cahn, R. W.; Flemings, M. C.; Ilschner, B.; Kramer, E. J.; Mahajan, S.; Veyssière, P. Eds.; Elsevier: Oxford, 2001; pp. 8986−8990, DOI: 10.1016/B0-08-043152-6/01620-X.

(12) Monpezat, A.; Couchaux, G.; Thomas, V.; Artheix, A.; Deliere, L.; Gréau, C.; Topin, S.; Coasne, B.; Roiban, L.; Cardenas, L.; Farrusseng, D. Effect of Chlorine-Containing VOCs on Silver Migration and Sintering in ZSM-5 Used in a TSA Process. *Catalysts* **2019**, *9*, 686.

(13) Monpezat, A.; Topin, S.; Thomas, V.; Pagis, C.; Aouine, M.; Burel, L.; Cardenas, L.; Tuel, A.; Malchère, A.; Epicier, T.; Farrusseng, D.; Roiban, L. Migration and Growth of Silver Nanoparticles in Zeolite Socony Mobil 5 (ZSM-5) Observed by Environmental Electron Microscopy: Implications for Heterogeneous Catalysis. *ACS Appl. Nano Mater.* **2019**, *2*, 6452−6461.

(14) Deliere, L.; Topin, S.; Coasne, B.; Fontaine, J.-P.; de Vito, S.; den Auwer, C.; Solari, P. L.; Daniel, C.; Schuurman, Y.; Farrusseng, D. Role of Silver Nanoparticles in Enhanced Xenon Adsorption Using Silver-Loaded Zeolites. *J. Phys. Chem. C* **2014**, *118*, 25032.

(15) Bethune, D. S.; Barker, J. A.; Rettner, C. T. Calculation of Desorption Rates for Xe/Pt(111) Using a Realistic Gas−Surface Potential. *J. Chem. Phys.* **1990**, *92*, 6847−6854.

(16) Clarke, S.; Bihlmayer, G.; Blügel, S. Chemical Effects in Rare Gas Adsorption: FLAPW Calculations for Ag (001)$c(2 \times 2)$-Xe. *Phys. Rev. B* **2001**, *63*, No. 085416.

(17) Chen, D.-L.; Al-Saidi, W. A.; Johnson, J. K. The Role of van Der Waals Interactions in the Adsorption of Noble Gases on Metal Surfaces. *J. Phys. Condens. Matter* **2012**, *24*, 424211.
(18) Waclawski, B. J.; Herbst, J. F. Photoemission for Xe Physisorbed on W(100): Evidence for Surface Crystal-Field Effects. *Phys. Rev. Lett.* **1975**, *35*, 1594−1596.
(19) Horn, K.; Scheffler, M.; Bradshaw, A. M. Photoemission from Physisorbed Xenon: Evidence for Lateral Interactions. *Phys. Rev. Lett.* **1978**, *41*, 822−825.
(20) Müller, N. Interaction of the Pt(111) Surface with Adsorbed Xe Atoms. *Phys. Rev. Lett.* **1990**, *65*, 3021−3024.
(21) Jamshidi, Z.; Far, M. F.; Maghari, A. Binding of Noble Metal Clusters with Rare Gas Atoms: Theoretical Investigation. *J. Phys. Chem. A* **2012**, *116*, 12510−12517.
(22) Lang, N. D. Interaction between Closed-Shell Systems and Metal Surfaces. *Phys. Rev. Lett.* **1981**, *46*, 842−845.
(23) Bader, R. F. W. *Atoms in Molecules: A Quantum Theory*; Clarendon Press: 1994.
(24) Unguris, J.; Bruch, L. W.; Moog, E. R.; Webb, M. B. Xe Adsorption on Ag(111): Experiment. *Surf. Sci.* **1979**, *87*, 415−436.
(25) Stoner, N.; Van Hove, M. A.; Tong, S. Y.; Webb, M. B. Dynamical Calculations of Low-Energy Electron Diffraction for Incommensurate Lattice Structures—Xe on Ag(111). *Phys. Rev. Lett.* **1978**, *40*, 243−246.
(26) Dai, P.; Wu, Z.; Angot, T.; Wang, S.-K.; Taub, H.; Ehrlich, S. N. Synchrotron X-Ray-Diffraction Study of the Structure and Growth of Xe Films Adsorbed on the Ag(111) Surface. *Phys. Rev. B: Condens. Matter* **1999**, *59*, 15464.
(27) McElhiney, G.; Papp, H.; Pritchard, J. The Adsorption of Xe and CO on Ag(111). *Surf. Sci.* **1976**, *54*, 617−634.
(28) Behm, R. J.; Brundle, C. R.; Wandelt, K. The Underlayer Influence on Photoemission and Thermal Desorption of Xenon Adsorbed on Ag(111). *J. Chem. Phys.* **1986**, *85*, 1061−1073.
(29) Gibson, K. D.; Sibener, S. J. Inelastic Helium Scattering Studies of Ordered Ar, Kr, and Xe Monolayers Physisorbed on Ag(111): Dispersion Curves, Scattering Cross Sections, and Excitation Line Shapes. *J. Chem. Phys.* **1988**, *88*, 7862−7892.
(30) Flores, M. A.; Menéndez-Proupin, E. Spin-Orbit Coupling Effects in Gold Clusters: The Case of Au13. *J. Phys. Conf. Ser.* **2016**, *720*, No. 012034.
(31) Shi, Y.-K.; Li, Z. H.; Fan, K.-N. Validation of Density Functional Methods for the Calculation of Small Gold Clusters. *J. Phys. Chem. A* **2010**, *114*, 10297−10308.
(32) Vidali, G.; Ihm, G.; Kim, H. Y.; Cole, M. W. Potentials of Physical Adsorption. *Surf. Sci. Rep.* **1991**, *12*, 135−181.
(33) Seyller, T.; Caragiu, M.; Diehl, R. D.; Kaukasoina, P.; Lindroos, M. Observation of Top-Site Adsorption for Xe on Cu(111). *Chem. Phys. Lett.* **1998**, *291*, 567−572.
(34) Schmidbaur, H. The Aurophilicity Phenomenon: A Decade of Experimental Findings, Theoretical Concepts and Emerging Applications. *Gold Bull.* **2000**, *33*, 3−10.
(35) Pyykkö, P. Strong Closed-Shell Interactions in Inorganic Chemistry. *Chem. Rev.* **1997**, *97*, 597−636.
(36) Kaltsoyannis, N. Relativistic Effects in Inorganic and Organometallic Chemistry. *J. Chem. Soc. Dalton Trans.* **1997**, *1*, 1−12.
(37) Faas, S.; Van Lenthe, J. H.; Snijders, J. G. Regular Approximated Scalar Relativistic Correlated Ab Initio Schemes: Applications to Rare Gas Dimers. *Mol. Phys.* **2000**, *98*, 1467−1472.
(38) Pereiro, M.; Baldomir, D. Structure of Small Silver Clusters and Static Response to an External Electric Field. *Phys. Rev. A* **2007**, *75*, No. 033202.
(39) Gonze, X.; Beuken, J.-M.; Caracas, R.; Detraux, F.; Fuchs, M.; Rignanese, G.-M.; Sindic, L.; Verstraete, M.; Zerah, G.; Jollet, F.; Torrent, M.; Roy, A.; Mikami, M.; Ghosez, P.; Raty, J.-Y.; Allan, D. C. First-Principles Computation of Material Properties: The ABINIT Software Project. *Comput. Mater. Sci.* **2002**, *25*, 478−492.
(40) Gonze, X.; Jollet, F.; Abreu Araujo, F.; Adams, D.; Amadon, B.; Applencourt, T.; Audouze, C.; Beuken, J.-M.; Bieder, J.; Bokhanchuk, A.; Bousquet, E.; Bruneval, F.; Caliste, D.; Côté, M.; Dahm, F.; Da Pieve, F.; Delaveau, M.; Di Gennaro, M.; Dorado, B.; Espejo, C.; Geneste, G.; Genovese, L.; Gerossier, A.; Giantomassi, M.; Gillet, Y.; Hamann, D. R.; He, L.; Jomard, G.; Laflamme Janssen, J.; Le Roux, S.; Levitt, A.; Lherbier, A.; Liu, F.; Lukačević, I.; Martin, A.; Martins, C.; Oliveira, M. J. T.; Poncé, S.; Pouillon, Y.; Rangel, T.; Rignanese, G.-M.; Romero, A. H.; Rousseau, B.; Rubel, O.; Shukri, A. A.; Stankovski, M.; Torrent, M.; Van Setten, M. J.; Van Troeye, B.; Verstraete, M. J.; Waroquiers, D.; Wiktor, J.; Xu, B.; Zhou, A.; Zwanziger, J. W. Recent Developments in the ABINIT Software Package. *Comput. Phys. Commun.* **2016**, *205*, 106−131.
(41) Perdew, J. P.; Burke, K.; Ernzerhof, M. Generalized Gradient Approximation Made Simple. *Phys. Rev. Lett.* **1996**, *77*, 3865−3868.
(42) Grimme, S.; Antony, J.; Ehrlich, S.; Krieg, H. A Consistent and Accurate Ab Initio Parametrization of Density Functional Dispersion Correction (DFT-D) for the 94 Elements H-Pu. *J. Chem. Phys.* **2010**, *132*, 154104.
(43) Holzwarth, N. A. W.; Tackett, A. R.; Matthews, G. E. A Projector Augmented Wave (PAW) Code for Electronic Structure Calculations, Part I: Atompaw for Generating Atom-Centered Functions. *Comput. Phys. Commun.* **2001**, *135*, 329−347.
(44) Pereiro, M.; Baldomir, D.; Arias, J. E. Unexpected Magnetism of Small Silver Clusters. *Phys. Rev. A* **2007**, *75*, No. 063204.
(45) Titantah, J. T.; Karttunen, M. Ab Initio Calculations of Optical Properties of Silver Clusters: Cross-over from Molecular to Nanoscale Behavior. *Eur. Phys. J. B* **2016**, *89*, 125.
(46) Rao, Y.; Lei, Y.; Cui, X.; Liu, Z.; Chen, F. Optical and Magnetic Properties of Cu-Doped 13-Atom Ag Nanoclusters. *J. Alloys Compd.* **2013**, *565*, 50−55.
(47) Longo, R. C.; Gallego, L. J. Structures of 13-Atom Clusters of Fcc Transition Metals by *Ab Initio* and Semiempirical Calculations. *Phys. Rev. B* **2006**, *74*, 193409.
(48) Sun, J.; Xie, X.; Cao, B.; Duan, H. A Density-Functional Theory Study of Au_{13}, Pt_{13}, $Au_{12}Pt$ and $Pt_{12}Au$ Clusters. *Comput. Theor. Chem.* **2017**, *1107*, 127−135.
(49) Michaelian, K.; Rendón, N.; Garzón, I. L. Structure and Energetics of Ni, Ag, and Au Nanoclusters. *Phys. Rev. B* **1999**, *60*, 2000−2010.
(50) Soini, T. M.; Ma, X.; Üzengi Aktürk, O.; Suthirakun, S.; Genest, A.; Rösch, N. Extending the Cluster Scaling Technique to Ruthenium Clusters with Hcp Structures. *Surf. Sci.* **2016**, *643*, 156−163.
(51) Fournier, R. Theoretical Study of the Structure of Silver Clusters. *J. Chem. Phys.* **2001**, *115*, 2165−2177.
(52) Lammers, U.; Borstel, G. Electronic and Atomic Structure of Copper Clusters. *Phys. Rev. B* **1994**, *49*, 17360−17377.
(53) Häberlen, O. D.; Chung, S.-C.; Stener, M.; Rösch, N. From Clusters to Bulk: A Relativistic Density Functional Investigation on a Series of Gold Clusters Au_n, N=6,...,147. *J. Chem. Phys.* **1997**, *106*, 5189−5201.

https://doi.org/10.1021/acsomega.1c03849
ACS Omega 2021, 6, 31513−31519